

# The Measurement of the Velocities of $P$ and $S$ Waves Propagating in the Surface Layer of Ice Sheet at Mizuho Station, East Antarctica

Kenji ISHIZAWA\*

みずほ基地における氷床表層部の  $P$  波  $S$  波の速度測定

石 沢 賢 二\*

**要旨：**南極大陸氷床上部の  $P$  波と  $S$  波の速度が、みずほ基地 ( $70^{\circ}42'S$ ,  $44^{\circ}20'E$ , 海拔 2230 m) において測定された。測定方法は、12・13次日本南極地域観測隊で掘削されたボーリング孔を使用した検層と、屈折法である。検層には孔中固着式受震器が使用され、深さ 80 m までの  $P$  波  $S$  波の速度構造が求められた。また屈折法では  $P$  波の構造が 36 m まで測定された。

得られた結果は、コアーを使用した超音波パルス法による測定結果とほぼ同じであった。

南極やグリーンランドのさまざまな場所で得られた  $P$  波の速度構造を対比してみた結果、その場所での年平均気温と強い相関があることがわかった。深さ 50 m の  $P$  波速度に注目してみると、年平均気温、 $T_m$  ( $^{\circ}C$ ), が高いほど  $P$  波の速度、 $V_P$  (km/s), は大きく、それらの間には次のような関係がある。

$$V_P = 0.034T_m + 4.529.$$

**Abstract:** The measurements of  $P$  and  $S$  wave velocity in the surface layer down to a depth of 80 m were made at Mizuho Station ( $70^{\circ}42'S$ ,  $44^{\circ}20'E$ , 2230 m a.s.l.) in 1978 by the following method: one was a borehole logging and the other was a refraction. The variation of the velocity with depth was obtained and it was found that the velocity obtained in the measurement was approximately equal to that obtained experimentally in a laboratory using the core samples drilled at Mizuho Station.

The data of  $P$  wave velocity measured in Antarctica and Greenland were summarized and the relationship between the  $P$  wave velocity at a depth of 50 m,  $V_P$ , and the mean annual temperature,  $T_m$ , was ob-

---

\* 国立極地研究所. National Institute of Polar Research, 9-10, Kaga 1-chome, Itabashi-ku, Tokyo 173

tained as follows:  $V_P = 0.034 T_m + 4.529$  (km/s).

## 1. Introduction

The velocity and attenuation of elastic waves in snow and ice are among the basic physical constants of ice sheet in Antarctica. The variation of seismic velocity with depth shows us the structure of snow and ice. Since the seismological investigation by ROBIN (1958), a number of investigations were carried out to know elastic characteristics of ice sheet. The measurements of seismic wave velocities of ice sheet by refraction were made by THIEL and OSTENSO (1961), and ETO (1971). KOHNEN and BENTLEY (1972) carried out the ultrasonic (28 kHz) velocity logging down to a depth of 1550 meters in the 2164-meter borehole drilled at Byrd Station, West Antarctica, and obtained the  $P$  wave velocity profile with depth. This is the first measurement by using a deep borehole in ice sheet. But the  $S$  wave velocity detection by logging has never been successful.

In the laboratory BENETT (1972) and YAMADA (1978) measured the ultrasonic wave velocities of  $P$  and  $S$  waves using ice samples drilled in the Antarctic ice sheet. Though YAMADA (1978) measured the ultrasonic wave velocity of ice core samples drilled at Mizuho Station ( $70^{\circ}42'S$ ,  $44^{\circ}20'E$ , 2230 m a.s.l.), any field measurements of the wave velocities have not been made at and near Mizuho Station. Since the elastic wave velocity in snow and ice depends upon temperature (KOHNEN, 1974) and pressure (GOW, 1971), the velocity should be measured by a field test because in the laboratory the temperature can be controlled but the pressure cannot be realized.

The purpose of the present study is to obtain the actual wave velocity and establish the logging system especially for the  $S$  wave measurement in the surface layer of ice sheet and to clarify  $P$  and  $S$  wave velocity profiles with depth at Mizuho Station. The downhole measurements by logging from the surface to the 80 m depth in the borehole drilled at Mizuho Station were carried out during the period from June 1978 to December 1978. A short-distance refraction prospecting was also carried out in the same period.

## 2. Preliminary Measurement

The  $P$  and  $S$  waves in logging are generated by hitting a wooden plate fixed at the snow surface vertically with a hammer and by hitting the end of

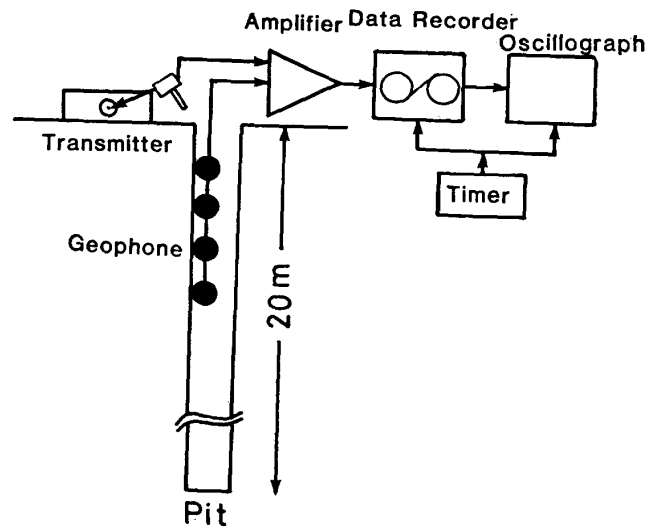


Fig. 1. Observation system in the 20 m deep pit.

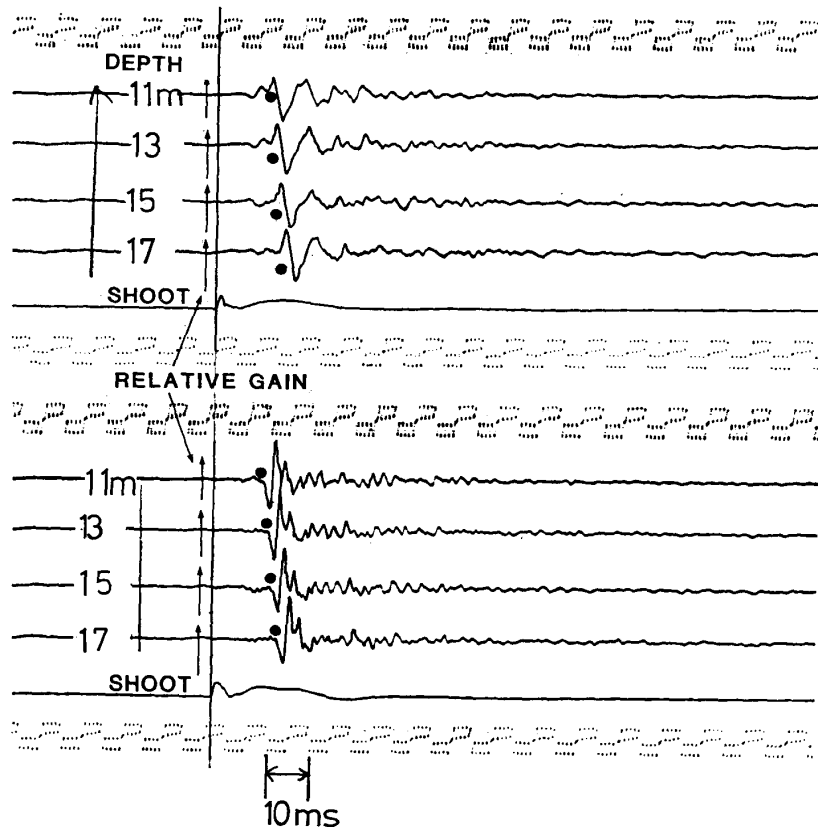


Fig. 2. A pair of *S* wave records in the 20 m deep pit. The polarities of the *S*-phases are reversed by reversing the hitting directions. Sensitivities of the respective traces are in proportion to the amplitudes of calibration signals attached at the beginning of the record.

the plate horizontally. The generation of pure *SH* wave is difficult because *SH* wave is generated only by a tangential stress on the snow surface. To detect *SH* wave, the hitting direction was reversed because *SH* wave changed its polarity when the direction of the tangential stress was reversed.

The preliminary tests were carried out by using a 20 m deep pit excavated at Mizuho Station. The experimental apparatus is outlined in Fig. 1. Four geophones with natural frequencies of 28 Hz (Ôyô, PS-5) were fixed to the snow wall horizontally at intervals of 2 m depth. *SH* wave was generated by hammer hitting the side of the plate in the direction of arrow as shown in Fig. 1.

As an example, a pair of the records obtained by the reverse blow of the hammer is shown in Fig. 2. Solid circles indicate the first arrivals of *SH* wave. Since the polarity of waves in the pair of records is clearly reversed by the reverse of hitting directions, the observed waves are confirmed to be *SH* wave.

### 3. Logging in Borehole

#### 3.1. Method

The *P* and *S* wave velocity logging was carried out in a borehole, 150 mm in diameter and 147.5 m in depth, drilled at Mizuho Station in 1971–1972. A fixed-type detector (KITSUNEZAKI, 1971) was used in the experiment. The detector consists of one vertical and two horizontal component geophones, but the sensor to detect a horizontal azimuth of the components is not installed. As shown in Fig. 3, the detector is fixed to the wall of the borehole by inflating a rubber tube with compressed

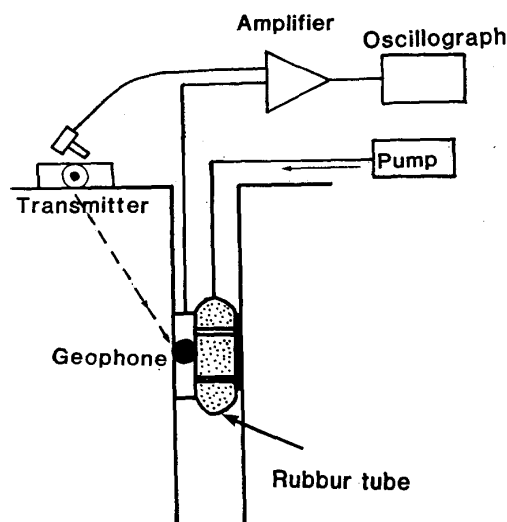


Fig. 3. Observation system in the borehole.

air of about  $2 \text{ kg/cm}^2$  supplied by a pump. *P* and *S* waves were generated by the same method as mentioned in Section 2, and were recorded from the snow surface down to the 80 m depth by replacing the detector at depth intervals of 2 m.

### 3.2. *P* and *S* wave velocity profiles with depth

Fig. 4 shows the results obtained at the 32 m depth from the top of the borehole. Each result was obtained by reversing the hitting direction to detect *SH* wave. The first trace is a shooting signal, the second is the wave detected by a horizontal component geophone at the 2 m depth, and the others indicated by V and H are the wave forms by one vertical and two horizontal component geophones at the 32 m depth. The polarity of first motions de-

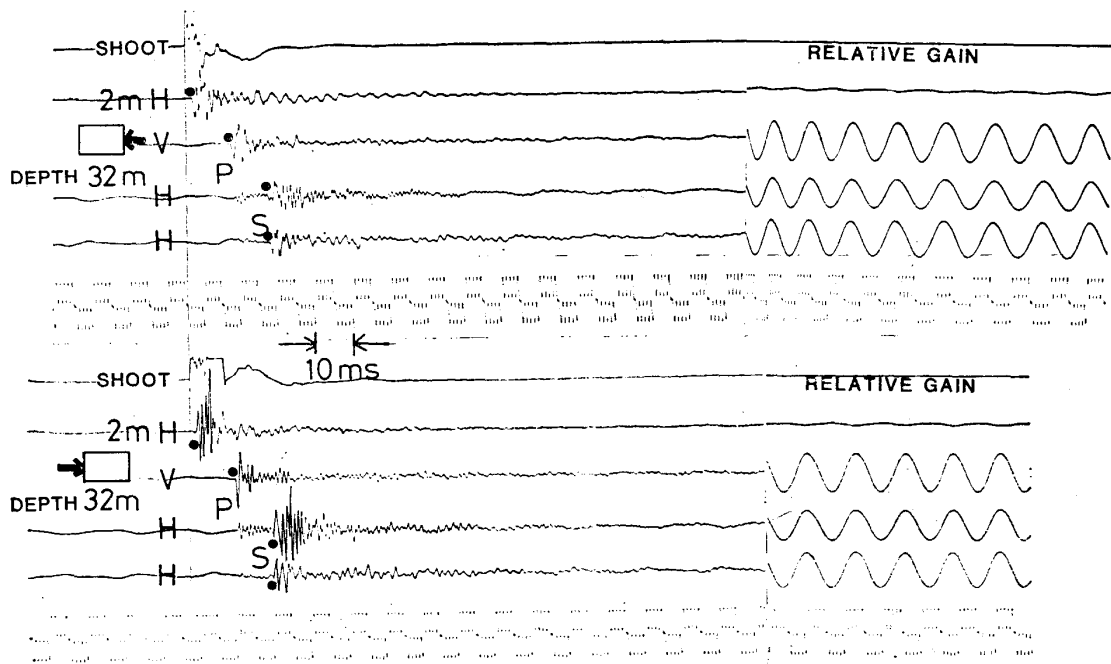


Fig. 4. A pair of *S* wave records in the borehole.

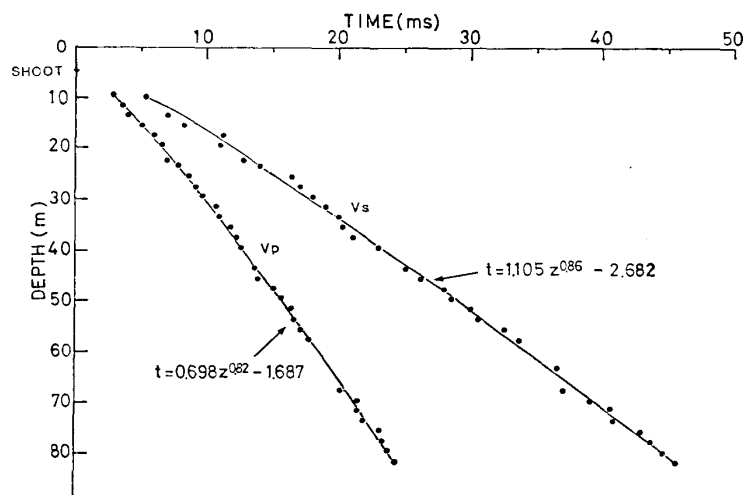


Fig. 5. Travel time versus depth for *P* and *S* waves.

ected by the 2 m depth geophone is reversed when the hitting direction is reversed, therefore *SH* wave is generated though its recorded form may be overlapped by *P* wave of a small amplitude. The amplitude of *S* wave is so large that its first arrivals can be detected obviously.

As is shown in Fig. 5 which illustrates the relation between the travel time of the waves and the depth, the travel time of *P* and *S* waves changes continuously with depth. The travel time,  $t$ , can be expressed by the following equation from the analysis of the data in Fig. 5.

$$t = aZ^b + c, \quad 7.6 \leq Z \leq 80 \text{ m}, \quad (3.1)$$

where  $Z$  is the depth from the surface and  $a$ ,  $b$  and  $c$  are constants determined by a non-linear regression analysis. For *S* wave

$$a = 1.105, \quad b = 0.857 \text{ and } c = -2.682. \quad (3.2)$$

For *P* wave,

$$a = 0.698, \quad b = 0.820 \text{ and } c = 1.687. \quad (3.3)$$

Elastic wave velocity,  $V(Z)$ , calculated from eq. (3.1) is given by the following equation:

$$V(Z) = \frac{dZ}{dt} = (abZ^{b-1})^{-1} \quad (3.4)$$

Substituting the values of  $a$  and  $b$  in eqs. (3.2) and (3.3), we obtain the *P* wave velocity,  $V_P$  (km/s), and the *S* wave velocity,  $V_S$  (km/s), for  $7.6 \leq Z \leq 80$  m as follows:

$$V_P = 1.747Z^{0.180} \quad (3.5)$$

$$V_S = 1.056Z^{0.143} \quad (3.6)$$

The obtained results of  $V_P$  and  $V_S$  dependence upon the depth are shown in

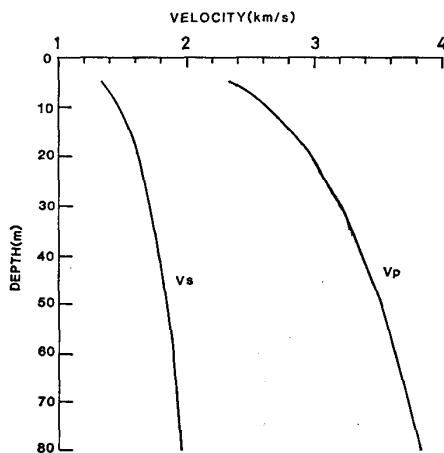


Fig. 6. *P* and *S* wave velocities by borehole logging.

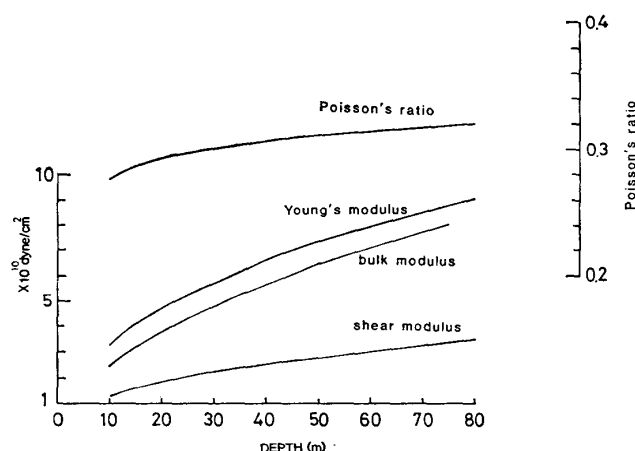


Fig. 7. Elastic constants calculated by using  $P$  and  $S$  wave velocities.

Fig. 6.  $P$  and  $S$  wave velocities between the surface and the 7.6 m depth are not measured. Fig. 6 shows that  $P$  and  $S$  wave velocities increase with depth continuously, and  $V_P$  and  $V_S$  at a depth of 80 m are 3.84 km/s and 1.98 km/s. Fig. 7 shows elastic constants calculated by using the results of  $V_P$  and  $V_S$ .

#### 4. $P$ Wave Velocities by Refraction Method

Since the velocities of the surface layer down to a depth of about 10 m were not obtained by logging, the  $P$  wave velocity profile was measured by a refraction method at Mizuho Station. The shooting was made by vertical hammer hitting of a concrete plate set on the snow surface at one end of the measurement line along which detectors were set. The detectors were the same as those used in logging in the 20 m deep pit.

An example of the obtained results and a travel time are shown in

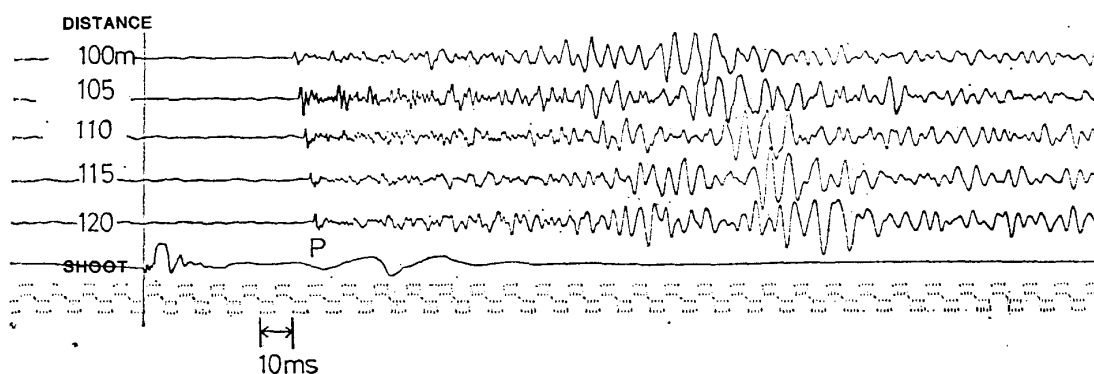


Fig. 8. An example of records by the refraction method.

Figs. 8 and 9.  $V_P$  can be obtained by using a numerical integration formula (SLICHTER, 1932):

$$Z_{x_1} = \frac{1}{\pi} \int_0^{x_1} \cosh^{-1} \left( \frac{V_{x_1}}{V_x} \right) dx \quad (4.1)$$

where  $Z_{x_1}$  is the depth corresponding to the velocity  $V_{x_1}$  and the maximum depth penetrated by the wave which first arrived at distance  $x_1$ . The equation is valid provided that the velocity increases gradually with depth between the surface and  $Z_{x_1}$ . Therefore, travel time,  $t$ , becomes a mono-increase function of  $x$ , and its differentiation,  $dt/dx = (V_x)^{-1}$ , becomes a mono-decrease

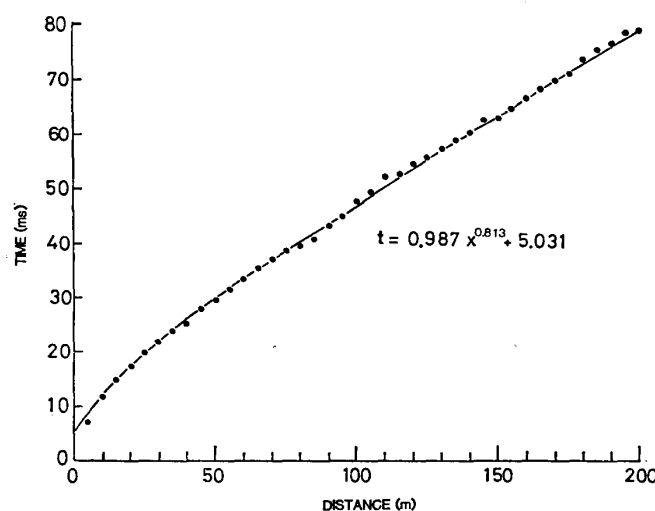


Fig. 9. Travel time versus distance plots in the refraction method.

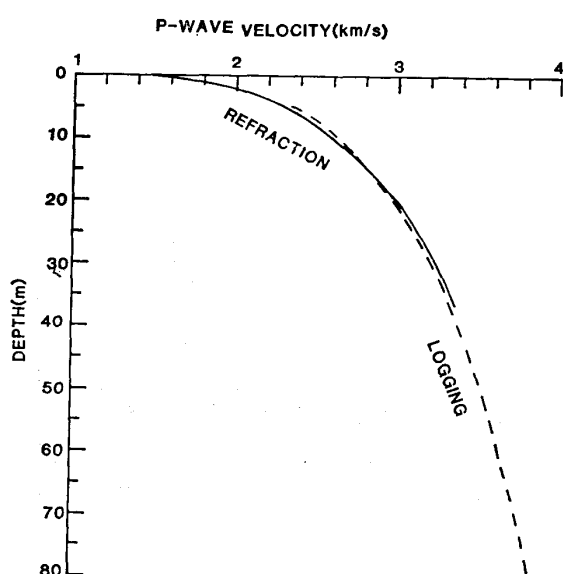


Fig. 10.  $P$  wave velocities obtained by the refraction method (solid line) and by logging (dashed line).



function of  $x$ . In order to satisfy the above conditions of a function of  $t$  and  $dt/dx$ , the following exponential equation is given from the obtained data:

$$t = ax^b + c \quad 5 \leq x \leq 200 \text{ m} \quad (4.2)$$

where  $a$ ,  $b$  and  $c$  are constants calculated by regression analysis. For the present measurement,

$$a = 0.987, b = 0.813 \text{ and } c = 5.031. \quad (4.3)$$

The calculated velocity profile with depth between the surface and 36.4 m is shown in Fig. 10. The results are almost the same as those obtained by logging.

## 5. Discussion

### 5.1. The relationship between $P$ and $S$ wave velocities and density

Since the investigation of ROBIN (1958), it is known that the elastic wave velocity of snow and/or ice is influenced by the density remarkably. Then, the density dependence of the wave velocity was investigated in the present study.

The density-depth profile at Mizuho Station is given by the following equation on the basis of core data given by NARITA and MAENO (1978):

$$\rho = 0.306 \log Z + 0.293 \quad 1 \leq Z \leq 80 \text{ m} \quad (5.1)$$

where  $\rho$  is the density ( $\text{g/cm}^3$ ) and  $Z$  is the depth (m). Substituting eq. (5.1) into eqs. (3.5) and (3.6), the following equations are given:

$$\rho = 1.702 \log V_P - 0.119 \quad 2.52 \leq V_P \leq 3.84 \text{ km/s} \quad (5.2)$$

$$\rho = 2.135 \log V_S + 0.243 \quad 1.41 \leq V_S \leq 1.98 \text{ km/s} \quad (5.3)$$

where  $\rho$  is the density ( $\text{g/cm}^3$ ) and  $V_P$ ,  $V_S$  (km/s) are the velocities of compressional and shear waves.

### 5.2. Comparison of $P$ and $S$ wave velocities with ultrasonic wave velocities obtained experimentally

YAMADA (1978) measured ultrasonic wave velocities of core samples obtained from the same borehole as the one used in the present study in a laboratory under a temperature condition of  $-10^\circ \pm 0.5^\circ \text{C}$ . His result is shown in Fig. 11 in which the result of the present study is illustrated. The both results show good agreement. The borehole temperature of the *in-situ* measurements is about  $-34^\circ \text{C}$  at the depth from 10 m to 80 m (FUJII, 1978). The temperature dependence of  $P$  and  $S$  wave velocities of ice was given as  $-2.3 \text{ m/s} \cdot ^\circ \text{C}$  and  $-1.2 \text{ m/s} \cdot ^\circ \text{C}$  by KOHNEN (1974). Since the temperature

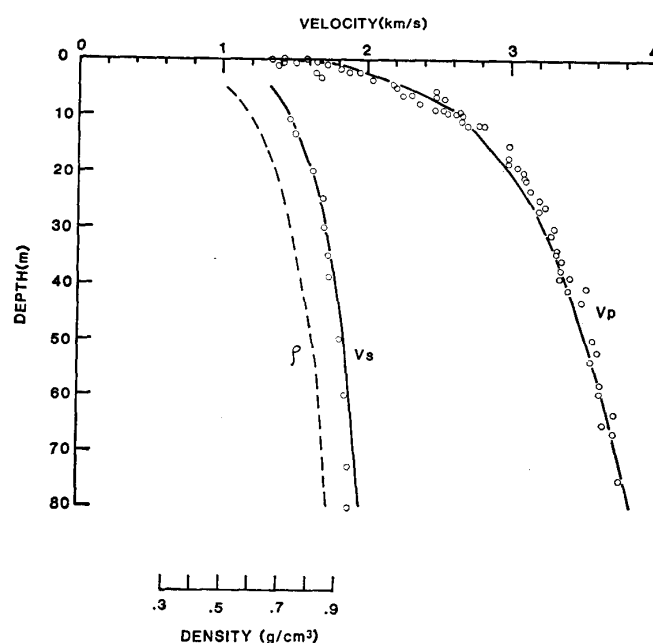


Fig. 11.  $P$  and  $S$  wave velocities in the *in-situ* (solid line) and in the laboratory (white circles) measurements. Dashed line denotes density of snow.

dependence of  $P$  and  $S$  wave velocity in snow has not been obtained, it is assumed that the wave velocity in snow has the same temperature dependence as that of ice. In this case, the velocity differences between the present result and YAMADA's one are expected to be 55.2 m/s and 28.8 m/s for  $P$  and  $S$  wave velocity respectively. But such difference cannot be found in Fig. 11. This may be explained by the fact that the error of  $P$  and  $S$  wave velocities in the present study is estimated to be  $\pm 50$  m/s from the accuracy of the present measurements.

Though in the laboratory measurement the core samples are considered to be released from an overburden pressure,  $P$  and  $S$  wave velocities obtained by the laboratory measurement coincide with those obtained by the *in-situ* measurement. This suggests that the elastic wave velocity gradients against the overburden pressure  $L$ ,  $dV_P/dL$  and  $dV_S/dL$  in a depth range from surface to 80 m are negligible.

### 5.3. Mean annual air temperature dependence of $P$ wave velocity

The elastic wave velocities in the Antarctic ice sheet depend on the

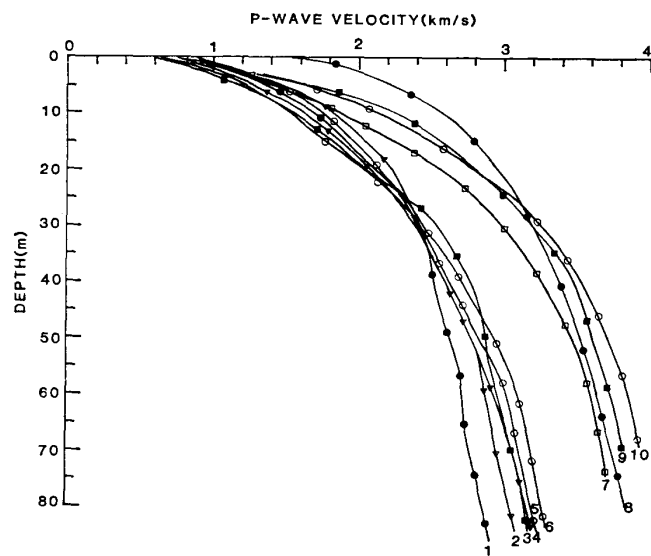


Fig. 12. Profiles of *P* wave velocities in the Antarctic ice sheet. The numbers under the lines denote locations of measurements summarized in Table 1.

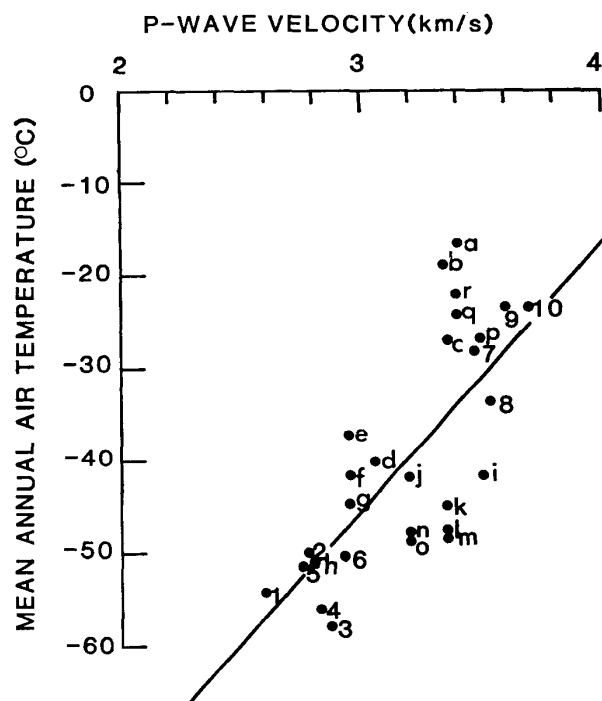


Fig. 13. Relationship between *P* wave velocities at 50m-depth and mean annual temperature. The numbers and letters correspond to those in Fig. 12 and Table 1.

density profile of snow which is attributed to climatic conditions such as snow accumulation rate and air temperature. In order to draw the map of *P* wave velocities in the polar regions, *P* wave velocities measured in Antarctica and Greenland were summarized. Fig. 12 shows the profiles of *P* wave velocities measured at various sites in the Antarctic ice sheet. As shown in this figure, the profiles in the depth range between 30 and 80 m are divided into two groups. That is, a higher velocity group measured in a coastal area and a lower one in an inland area.

*Table 1. Summary of the locations where P wave velocity profiles used for the comparison were measured.*

Symbols in Figs. 12 and 13	Location	References
1	75°57'S, 42°23'E	ETO (1971)
2	89°45'S, 42°14'E	ETO (1971)
3	77°26'S, 41°32'E	ETO (1971)
4	South Pole	WEIHAUPT (1963)
5	80°01'S, 40°39'E	ETO (1971)
6	85°03'S, 40°31'E	ETO (1971)
7	Byrd Station	KOHNEN and BENTLEY (1973)
8	Mizuho Station	ISHIZAWA (present study)
9	Ross Ice Shelf	KIRCHNER and BENTLEY (1979)
10	Filchner Ice Shelf	THIEL and BEHRENDT (1959)
a	Moudiheim	ROBIN (1958)
b	S 165 (near Moudiheim)	ROBIN (1958)
c	S 97 (near Moudiheim)	ROBIN (1958)
d	S 119 (near Moudiheim)	ROBIN (1958)
e	78°02'S, 159°20'E	CRARY (1963)
f	78°01'S, 158°25'E	CRARY (1963)
g	78°03'S, 152°45'E	CRARY (1963)
h	88°39'S, 157°30'W	CRARY (1963)
i	78°01'S, 155°18'E	CRARY (1963)
j	72°07'S, 148°12'E	CRARY (1963)
k	80°10'S, 139°02'E	CRARY (1963)
l	78°04'S, 139°32'E	CRARY (1963)
m	78°02'S, 145°13'E	CRARY (1963)
n	75°47'S, 148°27'E	CRARY (1963)
o	75°12'S, 146°49'E	CRARY (1963)
p	Site 2 (Greenland)	BENETT (1972)
q	Camp century (Greenland)	BENETT (1972)
r	Antarctic Peninsula	BEHRENDT (1963)

*P* wave velocities at 50m-depth *versus* mean annual air temperature are summarized and plotted in Fig. 13. *P* wave velocity at 50m-depth seems to be characterized by snow densification clearly, because the values at the snow surface are not much different by sites, and the *P* wave velocities at deeper depths than 80 m approach the velocity of ice, 3.9 km/s. In Fig. 13, the solid circles with symbols are summarized data (locations are compiled in Table 1), and a solid line is calculated by the least-squares of these values. Fluctuation of the plotted values may be caused by the difference of accumulation rate at each site. The relationship between *P* wave velocity of 50m-depth,  $V_P$  (km/s), and mean annual temperature,  $T_m$  ( $^{\circ}\text{C}$ ), is expressed by the solid line in Fig. 13 and is given by

$$V_P = 0.034T_m + 4.529 \quad (5.4)$$

The correlation coefficient of the above equation is 0.73.

### Acknowledgments

The kind cooperation given by the members of the 19th Japanese Antarctic Research Expedition led by Prof. T. HIRASAWA in the field observations under the severe meteorological condition is gratefully acknowledged. I am deeply indebted to Drs. C. KITSUNEZAKI and K. NORITOMI of Mining college of Akita University for discussing the observation system and the data analysis. Also I am grateful to Drs. S. MAE and Y. FUJII of the National Institute of Polar Research for reading the manuscript and providing constructive comments.

### References

- BEHRENDT, J. C. (1963): Seismic measurements on the ice sheet of the Antarctic Peninsula. *J. Geophys. Res.*, **68**, 5973-5990.
- BENNETT, H. F. (1972): Measurements of ultrasonic wave velocities in ice cores from Greenland and Antarctica. *CRREL Res. Rep.*, **237**, 55.
- BENTLEY, C. R. (1972): Seismic-wave velocities in anisotropic ice: A comparison of measured and calculated values in and around the deep drill hole at Byrd Station, Antarctica. *J. Geophys. Res.*, **77**, 4406-4420.
- ETO, T. (1971): Seismic studies during the JARE South Pole Traverse 1968-1969. *JARE Sci. Rep., Spec. Issue*, **2**, 115-124.
- FUJII, Y. (1978): Temperature profile in the drilled hole. *Mem. Natl Inst. Polar Res., Spec. Issue*, **10**, 169.
- GOW, A. J. (1971): Relaxation of ice in deep drill cores from Antarctica. *J. Geophys. Res.*, **76**, 2533-2541.

- KITSUNEZAKI, C. (1971): Field-experimental studies of Shear wave and the related problems. *Contrib. Geophys. Inst. Kyoto Univ.*, **11**, 103-177.
- KOHNEN, H. (1974): The temperature dependence of seismic waves in ice. *J. Glaciol.* **13**, 144-147.
- KOHNEN, H. and BENTLEY, C. R. (1973): Seismic refraction and reflection measurements at "Byrd" Station, Antarctica. *J. Glaciol.*, **12**, 101-111.
- NARITA, H. and MAENO, N. (1978): Compiled density data from cores drilled at Mizuho Station. *Mem. Natl Inst. Polar Res., Spec. Issue*, **10**, 136-158.
- ROBIN, G. de Q. (1958): Seismic shooting and related investigations. *Sci. Results, Norw.-Br.-Swed. Antarct. Exped. 1949-1952*, **5** (Glaciol. III), 162 p.
- SLICHTER, L. B. (1932): The theory of the interpretation of seismic travel-time curves in horizontal structure. *Phys.*, **3**, 273-295.
- THIEL, E. and BEHRENDT, J. C. (1959): Seismic studies on the Filchner ice shelf, Antarctica, 1957-1959. *IGY Glaciol. Rep. Ser.*, **2**, V-1-V-14.
- THIEL, E. and OSTENSO, N. A. (1961): Seismic studies on Antarctic ice shelves. *Geophys.*, **26**, 706-715.
- WEIHAUPT, J. G. (1963): Seismic and gravity studies at the South Pole. *Geophys.*, **28**, 582-592.
- YAMADA, T. (1978): Anisotropy of ultrasonic wave velocities in Mizuho cores. *Mem. Natl Inst. Polar Res., Spec. Issue*, **10**, 114-123.

*(Received April 9, 1981)*